D-3

LA-2449

LOS ALAMOS SCIENTIFIC LABORATORY

OF THE UNIVERSITY OF CALIFORNIA o LOS ALAMOS NEW MEXICO

THE FLOW OF FLUIDS THROUGH CHANNELS WITH POROUS WALLS

Index:
(1) Fluid Dynamics
(2) Gasdynamics

12/79

LEGAL NOTICE

This report was prepared as an account of Government sponsored work. Neither the United States, nor the Commission, nor any person acting on behalf of the Commission:

A. Makes any warranty or representation, expressed or implied, with respect to the accuracy, completeness, or usefulness of the information contained in this report, or that the use of any information, apparatus, method, or process disclosed in this report may not infringe privately owned rights; or

B. Assumes any liabilities with respect to the use of, or for damages resulting from the use of any information, apparatus, method, or process disclosed in this report.

As used in the above, "person acting on behalf of the Commission" includes any employee or contractor of the Commission, or employee of such contractor, to the extent that such employee or contractor of the Commission, or employee of such contractor prepares, disseminates, or provides access to, any information pursuant to his employment or contract with the Commission, or his employment with such contractor.

~~Printed in USA. Price $ .75.~~ Available from the

Office of Technical Services
U. S. Department of Commerce
Washington 25, D. C.

LA-2449
PHYSICS AND MATHEMATICS
TID-4500, 15th Ed.

LOS ALAMOS SCIENTIFIC LABORATORY
OF THE UNIVERSITY OF CALIFORNIA LOS ALAMOS NEW MEXICO

REPORT WRITTEN: July 1960

REPORT DISTRIBUTED: September 23, 1960

THE FLOW OF FLUIDS THROUGH CHANNELS WITH POROUS WALLS

by

Francisco A. Guevara
William E. Wageman

Contract W-7405-ENG. 36 with the U. S. Atomic Energy Commission

ABSTRACT

Approximate solutions of the equations of motion governing laminar incompressible fluid flow through a cylindrical channel with a porous wall are derived. The invalidity of an approximation in the solution of these equations under certain circumstances is pointed out, and the results of a numerical integration in the region where the approximation is invalid are indicated. A description is given of an experiment to verify the calculations, and some interesting results are noted.

ACKNOWLEDGMENTS

The authors would like to thank R. M. Potter for his assistance with the experimental work, B. W. Knight and B. B. McInteer for their enlightening and valuable contributions to the theoretical work, and E. S. Robinson for his continued encouragement in what turned out to be a long and difficult job.

CONTENTS

ILLUSTRATIONS

TABLE

INTRODUCTION

The flow of fluids through channels with porous walls has been of interest in the last decade or so because of applications to transpiration cooling, gaseous diffusion, and boundary-layer control. Several investigators[1-6] have contributed much to the theoretical study of this type of flow, but little has been done experimentally.

In general, the theoretical studies have been limited to laminar, incompressible flow. Most of the work has been done on the problem of a rectangular channel, and some interesting techniques have been developed for the solution of this problem. However, in this case it is rather difficult to check the solutions by a reasonably precise experiment.

We chose the more practical experimental problem of flow through a finite porous cylindrical tube, accepting the theoretical difficulties which are presented.

THEORY

Laminar, incompressible fluid flow through a channel with porous walls is governed by the specialized Navier-Stokes equations, the equation of continuity, and appropriate boundary conditions.

$$\rho(\vec{v}\cdot\nabla)\vec{v} - \eta(\nabla\cdot\nabla)\vec{v} + \nabla p = 0,$$

$$\nabla\cdot\vec{v} = 0.$$

ρ is the density of the fluid and η is its viscosity.

For a cylindrical channel with a uniformly porous wall the problem reduces to a two-dimensional one described by the following equations:

$$\rho\left(u\frac{\partial u}{\partial r} + v\frac{\partial u}{\partial z}\right) - \eta\left(\frac{\partial^2 u}{\partial r^2} + \frac{1}{r}\frac{\partial u}{\partial r} - \frac{u}{r^2} + \frac{\partial^2 u}{\partial z^2}\right) + \frac{\partial p}{\partial r} = 0,$$

$$\rho\left(u\frac{\partial v}{\partial r} + v\frac{\partial v}{\partial z}\right) - \eta\left(\frac{\partial^2 v}{\partial r^2} + \frac{1}{r}\frac{\partial v}{\partial r} + \frac{\partial^2 v}{\partial z^2}\right) + \frac{\partial p}{\partial z} = 0,$$

$$\frac{\partial}{\partial r}(ru) + \frac{\partial}{\partial z}(rv) = 0.$$

$u = u(r,z)$ is the radial component of the velocity, and $v = v(r,z)$ is the axial, or z-component of the velocity.

The boundary conditions arise from the following physical considerations. Because of symmetry there should be no radial velocity on the

axis of the tube, i.e. $u(o,z) = 0$. The axial velocity profile must be flat at the center of the tube, so $\left.\frac{\partial v}{\partial r}\right|_{r = o} = 0$. At the wall of the channel ($r = a$) the velocity should have only a radial component. Thus, $v(a,z) = 0$. If the flow density is the same through all portions of the porous wall, $u(a,z) = u_o$.

The analysis is simplified by the transformations $R = r/a$, $Z = z/a$, $P = p/\rho u_o^2$, $V = - v/u_o$, $U = - u/u_o$, and $\epsilon = - \eta/\rho u_o a$, which give the following dimensionless equations:

$$(U\frac{\partial U}{\partial R} + V\frac{\partial U}{\partial Z}) - \epsilon(\frac{\partial^2 U}{\partial R^2} + \frac{1}{R}\frac{\partial U}{\partial R} - \frac{U}{R^2} + \frac{\partial^2 U}{\partial Z^2}) + \frac{\partial P}{\partial R} = 0 ,$$

$$(U\frac{\partial V}{\partial R} + V\frac{\partial V}{\partial Z}) - \epsilon(\frac{\partial^2 V}{\partial R^2} + \frac{1}{R}\frac{\partial V}{\partial R} + \frac{\partial^2 V}{\partial Z^2}) + \frac{\partial P}{\partial Z} = 0 ,$$

$$\frac{\partial}{\partial R}(RU) + \frac{\partial}{\partial Z}(RV) = 0 .$$

The boundary conditions become $V(1,Z) = 0$, $U(1,Z) = -1$, $U(0,Z) = 0$, and $\left.\frac{\partial V}{\partial R}\right|_{R = 0} = 0$.

A consequence of the assumption that the flow density at the porous wall is uniform is that the Z-component of the velocity may be written as Z times some function of R, with $Z = 0$ defined by the point at which $V(R,Z) = 0$. By using this result and introducing a stream function ψ that identically satisfies the continuity equation, $RV = \frac{\partial \psi}{\partial R}$, $- RU = \frac{\partial \psi}{\partial Z}$, it is found that the expression for the pressure has the form

$P = P_o(R) + \frac{1}{2}\gamma Z^2$, where γ is a constant for a particular value of the parameter ϵ. $P_o(R)$ may be determined explicitly once the differential equations have been integrated.

A particular stream function which satisfies the continuity equation identically and also fits the boundary conditions is $\psi = BZf(R^2)$, where B is a constant. The argument of the function f is chosen to be R^2 rather than R for convenience in analysis.

The substitution $X = R^2$ gives $\psi = BZf(X)$, $U = -\frac{B}{\sqrt{X}}f(X)$, and $V = 2BZf'(X)$, where the prime denotes differentiation with respect to the argument of the function, which in this case is X. The velocity profile is given by V(X).

With the above expressions for U and V the differential equations become

$$\frac{2B^2}{\sqrt{X}}ff' - \frac{B^2}{X^{3/2}}f^2 + 4\epsilon B\sqrt{X}\, f'' + 2\sqrt{X}\, P_o' = 0, \qquad (1)$$

and

$$B^2(ff'' - f'^2) + 2\epsilon B(f'' + Xf''') = \frac{\gamma}{4}\ . \qquad (2)$$

If f is known explicitly, then P_o is determined within a constant of integration.

$$P_o = -B^2\int\frac{ff'}{X}\,dX + \frac{B^2}{2}\int\frac{f^2}{X^2}\,dX - 2\epsilon Bf' + K.$$

Equation (2) may be re-formulated for attack in two limiting cases. In the limit of large ϵ

$$\frac{2}{B}(f'' + Xf''') - \frac{1}{\epsilon}(f'^2 - ff'') = \frac{\gamma}{4\epsilon B^2} = d. \qquad (3)$$

This may be regarded as the equation governing the flow of fluids with high viscosities, or as the equation governing very slow flows. For high flows or small viscosities the limit of small ϵ gives

$$f'^2 - ff'' - \frac{2\epsilon}{B}(f'' + Xf''') = -\frac{\gamma}{4B^2} = c. \qquad (4)$$

Equations (3) and (4) are subject to the boundary conditions $f'(1) = 0$, $f(1) = \frac{1}{B}$, $\lim_{X\to 0} \frac{f(X)}{\sqrt{X}} = 0$, and $\lim_{X\to 0} \sqrt{X}\, f''(X) = 0$.

Equation (3) may be expanded around $(1/\epsilon) = 0$ to obtain a power series solution in $(1/\epsilon)$. Since γ may be a function of ϵ, d must also be expanded around $(1/\epsilon) = 0$. For greater clarity the solution of equation (3) will be denoted by $g(X)$, while the solution of equation (4) will remain $f(X)$.

$$g = g_o + \frac{1}{\epsilon}g_1 + \frac{1}{\epsilon^2}g_2 + \cdots,$$

$$d = d_o + \frac{1}{\epsilon}d_1 + \frac{1}{\epsilon^2}d_2 + \cdots.$$

For this series expansion the boundary conditions become

$$g_o(1) = \frac{1}{B}, \qquad g_n(1) = 0,\ n \geq 1,$$

$$g_n'(1) = 0,\ n \geq 0, \qquad \lim_{X\to 0} \frac{g_n(X)}{\sqrt{X}} = 0,\ n \geq 0,$$

$$\lim_{X\to 0} \sqrt{X}\, g_n''(X) = 0,\ n \geq 0.$$

Equation (3) has been solved to order $1/\epsilon^3$, but the solution is too unwieldy to present here. To order $1/\epsilon^2$

$$Bg(X) = -(X^2 - 2X) + \frac{1}{\epsilon}\left(\frac{X^4}{36} - \frac{X^3}{6} + \frac{X^2}{4} - \frac{X}{9}\right) - \frac{1}{\epsilon^2}\left(\frac{X^6}{5400} - \frac{X^5}{360} + \frac{X^4}{72}\right.$$

$$\left. - \frac{11X^3}{216} + \frac{19X^2}{270} - \frac{83X}{2700}\right) + \ldots ,$$

and $\gamma = -16\epsilon - 12 + \frac{88}{135}\frac{1}{\epsilon} - \frac{187}{315}\frac{1}{\epsilon^2} + \ldots .$

In a like manner equation (4) may be expanded around $\epsilon = 0$.

$$f = f_o + \epsilon f_1 + \epsilon^2 f_2 + \ldots ,$$

$$c = c_o + \epsilon c_1 + \epsilon^2 c_2 + \ldots .$$

A similar set of boundary conditions holds.

To zero order in ϵ equation (4) has the solutions

$f_o = \frac{(-1)^n}{B} \sin\left\{\frac{(2n + 1)\pi X}{2}\right\}$, $n = 0, 1, 2, \ldots .$ Recall that $X = R^2 = r^2/a^2$. These functions give a corresponding $\gamma = -(2n + 1)^2\pi^2$. The fact that there are an infinity of solutions may be tied in with the boundary condition at the exit end of the tube. The only solution that has been seen experimentally is that for which $n = 0$.

The solution of equation (4) has been carried out to order one in ϵ.[2] For the flows investigated the contribution of the first order term is small. At the lowest flow (largest ϵ) which gives useful data this term gives less than a 1% correction, and its effect decreases with decreasing ϵ.

It should be pointed out that the zero order small ϵ approximation amounts to neglecting the highest order derivative, and this term may or

may not be important. Numerical integration of an analogous problem shows that this procedure is valid when the wall is a source ($u_o < 0$), but that the highest order derivative dominates near the wall when there is suction ($u_o > 0$). In the limit of very high flows for wall suction the solution is $f = X/B$. This solution does satisfy the boundary conditions and gives a value of γ of -4.

APPARATUS

Two separate sets of experiments were performed in an effort to check the theoretical predictions. The first set yielded qualitative agreement with the theory and information necessary for the design of the second, more quantitative set of experiments. The porous system used in the early experiments, shown in Fig. 1, consisted of an alundum tube which was jacketed by a brass cylinder. Six pressure probes evenly spaced along the length of the alundum tube at its inside wall were used to measure the pressure drop down the channel. Differential measurements of pressure against the pressure at the top of the tube on its axis were read on a water manometer system.

This system qualitatively verified the parabolic pressure profile ($P = \frac{1}{2}\gamma Z^2$), but quantitative verification ($\gamma = -\pi^2$) was not possible. Also, attempts to measure the velocity profile proved futile because of the small size of the channel. A larger porous tube that more nearly satisfied the theoretical assumptions had to be found.

The main criteria in selecting a porous tube were that the material must have uniform porosity and that it present a suitably large impedance to the flow. Graphite, electroplated metal screen, pressed metal screen,

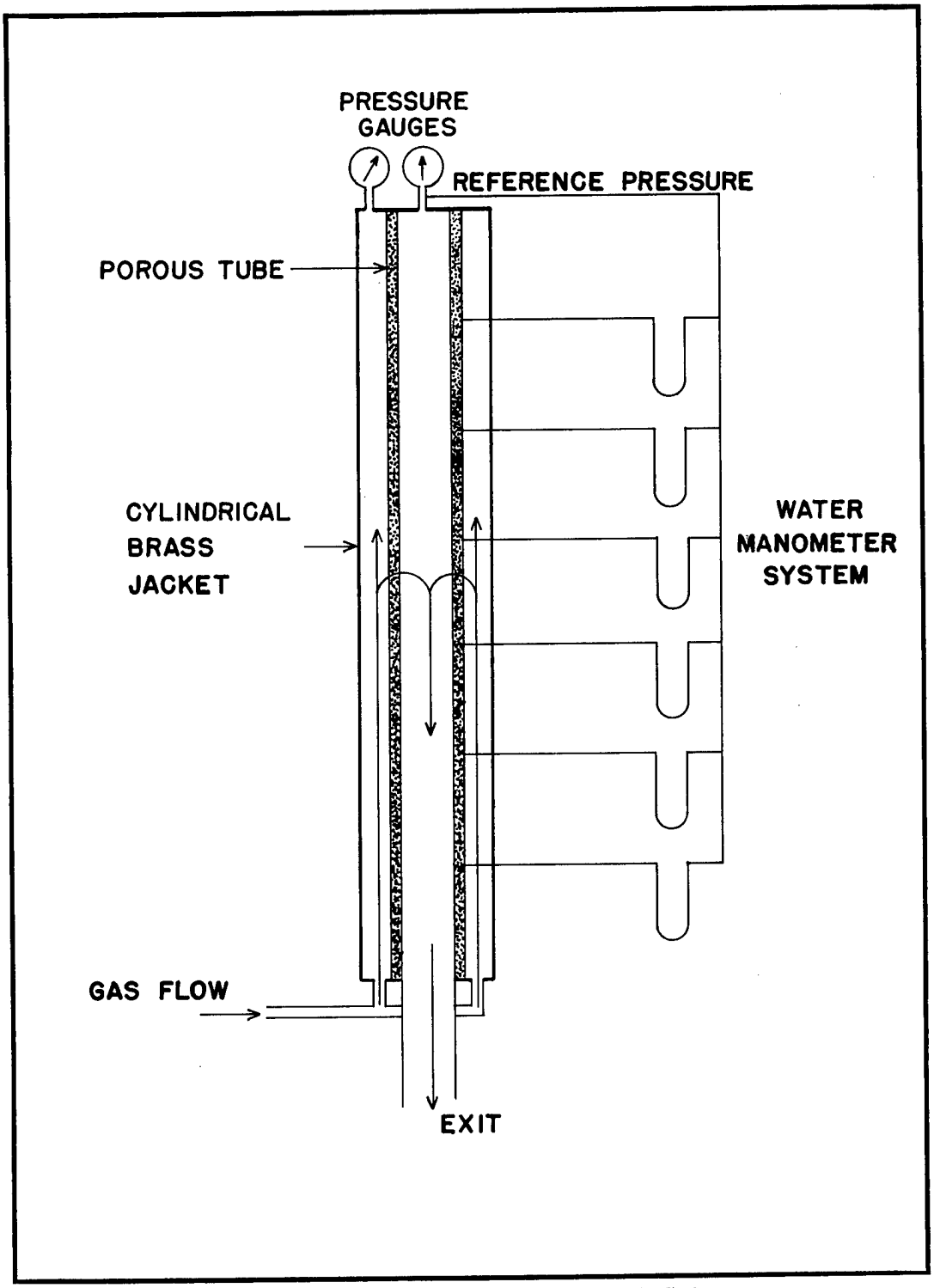

Fig. 1 - Schematic of Experimental Setup

sintered metal powder, filter paper, and several forms of alundum refractory were tested for these characteristics. Alundum was chosen again for the final experiments because, of the readily available materials, it most nearly satisfied the requirements. A thicker-walled tube was selected so the impedance would be large enough.

The tube in the modified apparatus was 18 inches long and had a $1\frac{1}{2}$ inch bore and a $\frac{1}{4}$ inch wall. Pressure probes to measure γ were installed only at the top and bottom of the channel. Measurements of the velocity profile were made by a pair of differential impact tubes which faced into the gas stream. These are shown in Fig. 2. One of the tubes was fixed on the channel axis and the other was adjustable radially. The impact tubes were mounted in a holder to form a unit which was movable along the length of the channel. Accurate knowledge of the radial position of the movable probe was lost if the unit was moved away from the bottom of the tube.

In both experiments the gas flow was up from the bottom of the vertical unit, through the porous wall, and back to the bottom where it was discharged to the atmosphere.

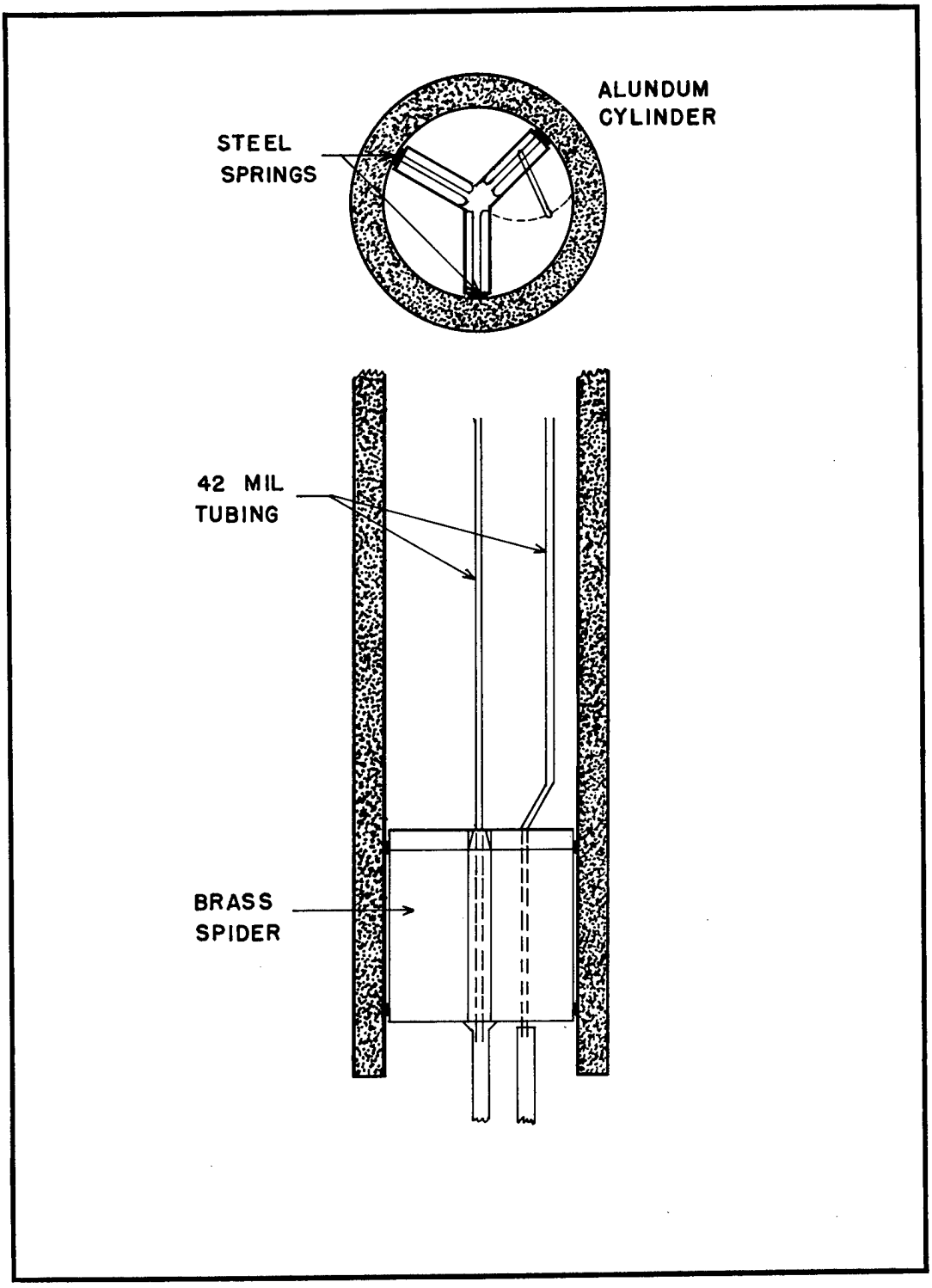

Fig. 2 - Velocity Profile Impact Tubes

RESULTS

The limiting value of the parameter γ and the magnitude and shape of the velocity profile are the only things that have been successfully checked experimentally, and these were found only in the case of small ϵ (large flows). Experimental error was too great to allow a determination of γ as a function of ϵ, and the sensitivity of the measurements could not be made high enough to give meaningful results at low flows.

The theory shows that when the wall is a source ($u_o < 0$) γ should have a limiting value of $-\pi^2$, and the velocity profile should be given by

$$V = 2BZf'(X) = \pi Z \cos\left\{\frac{\pi}{2} X\right\} .$$

The axial velocity as a function of the position variables is then

$$v = -\frac{\pi u_o z}{a} \cos\left\{\frac{\pi}{2}\left[\frac{r}{a}\right]^2\right\} .$$

γ and v must now be expressed in terms of measurable quantities.

Note that $\gamma = 2\Delta P/Z^2$, where $\Delta P = \Delta p/\rho u_o^2$ and $Z = z/a$. Therefore $\gamma = \dfrac{2a^2\Delta p}{\rho u_o^2 z^2}$. u_o may be expressed in terms of the total measured flow, Q, in gm/sec, through a conservation of mass relationship. If L is the

length of the porous tube, the mass of fluid into the wall each second between z = 0 and arbitrary z is Qz/L. The quantity out of the wall every second is JA, where J is the flow density, $-\rho u_o$, and A is the cylindrical area of the wall section considered. Thus

$$Qz/L = JA = -\rho u_o 2\pi a z,$$

and

$$\rho u_o^2 = \frac{Q^2}{4\pi^2 a^2 L^2 \rho} .$$

This gives the expression $\gamma = 8\pi^2 a^4 L^2 \rho \Delta p / Q^2 z^2$. In the experiment Δp is the pressure difference between the points z = L and z = 0. Therefore

$$\gamma = 8\pi^2 a^4 \rho \frac{\Delta p}{Q^2} . \qquad (5)$$

Δp, and hence γ, can be shown to be a negative number by considering Bernoulli's Law along a streamline.

The differential impact tubes measure the difference

$$\Delta P_r = P_o - P_r = \tfrac{1}{2}\rho(v_o^2 - v_r^2) ,$$

where v_o and v_r are the fluid velocities in the axial direction on the axis and at an arbitrary radial position, respectively. Since it is inconvenient to measure v_o for each flow, and since the velocity at the wall, v_w, is small, v_o is eliminated in favor of v_w.

$$\Delta P_w = P_o - P_w = \tfrac{1}{2}\rho(v_o^2 - v_w^2).$$

Thus, $v_r = \sqrt{\frac{2}{\rho}} \sqrt{\Delta P_w - \Delta P_r - P_w}$. In the experiment P_w was found to be negligibly small, so the velocity profile is expressible in terms of two differential pressure measurements:

$$v_r = \sqrt{\frac{2}{\rho}} \sqrt{\Delta P_w - \Delta P_r} \quad . \tag{6}$$

The subscript on the ΔP's indicates the position of the movable impact tube.

Comparison of theory and experiment for the velocity profile is facilitated if the shape and amplitude of the profile are given separately. For the shape, equation (6) is normalized so the data may be directly compared with $\cos\left\{\frac{\pi}{2}\left[\frac{r}{a}\right]^2\right\}$. The theoretical amplitude is

$$v_{o_t} = -\frac{\pi u_o z}{a} = \frac{Q\frac{z}{L}}{2\rho a^2} \quad , \tag{7}$$

and the experimental amplitude is given by the normalizing factor

$$v_{o_e} = \sqrt{\frac{2}{\rho}} \sqrt{\Delta P_w} \quad .$$

When the wall is a sink ($u_o > 0$) the boundary-layer type of flow that results has a flat velocity profile (except near the wall). γ may be calculated knowing that $\Delta p/\rho\bar{v}^2 = -\frac{1}{2}$ for this type of profile. Using a mass balance equation for the axial direction, $Qz/L = JA = \rho\bar{v}\pi a^2$.

$$\frac{\Delta p}{\rho\bar{v}^2} = \pi^2 a^4 L^2 \rho \frac{\Delta p}{Q^2 z^2} = \frac{\gamma}{8} = -\frac{1}{2} \quad .$$

It is seen that $\gamma = -4$ for $u_o > 0$.

All quantities in equations (5), (6), and (7) are in cgs units. However, since it is more convenient to measure Δp and the ΔP's in units of mm of water, a correction factor of $98 \frac{\text{dynes/cm}^2}{\text{mm of water}}$ must be introduced. This, along with the $19\frac{1}{4}$ mm radius of the porous tube, gives the results

$$\gamma = 1.063 \times 10^5 \rho \frac{\Delta p}{Q^2} \quad , \tag{5a}$$

$$v_r = \frac{14}{\sqrt{\rho}} \sqrt{\Delta P_w - \Delta P_r} \quad , \tag{6a}$$

$$v_{o_t} = \frac{0.1349}{\rho} Q \frac{z}{L} \quad . \tag{7a}$$

When the wall is a source, ρ is the density of the gas used (nitrogen) at room temperature and Los Alamos atmospheric pressure. This density is 0.970×10^{-3} gm/cm^3. Thus

$$\gamma = 103 \frac{\Delta p}{Q^2} \quad , \tag{5b}$$

$$v_r = 449.5 \sqrt{\Delta P_w - \Delta P_r} \quad , \tag{6b}$$

$$v_{o_t} = 139 \, Q \frac{z}{L} \quad . \tag{7b}$$

The Δp and the ΔP's are in mm of water.

Only γ may be checked quantitatively when the wall is a sink, and in this case an additional measurement to find the density of the gas must be made. In terms of the absolute operating pressure inside the porous tube, Π, psi,

$$\gamma = 9.05 \Pi \frac{\Delta p}{Q^2} \quad . \tag{5c}$$

The experimental values of γ were close to the theoretically predicted values for both flow directions. It was found that when the wall is a sink, $\gamma = -3.88 \pm 0.08$ (-4.00 was predicted from the theory), and when the wall is a source, $\gamma = -9.88 \pm 0.11$ (-9.87 was predicted).

These results are the averages of 15 and 14 determinations, respectively, with standard deviations, over a range of flows from 5.84 to 47.7 gm/sec of nitrogen. The experiments were done at a pressure of 11.6 psia and a temperature of about 25°C.

The amplitude of the velocity profile for $u_o > 0$ could not be found experimentally, but the flat character of this profile was verified within the sensitivity of our pressure measuring system (a water manometer).

The velocity profile data for $u_o < 0$ are presented in Table 1, with a "typical" set superimposed on the theoretical profile in Fig. 3. Experimental precision on the steep slope portion of the curve was not as high as on the flatter portions because small errors in knowledge of the position of the movable probe change the value of the cosine considerably. This introduced considerable experimental error when the probes were moved away from the bottom of the tube ($z/L = 1$).

In Table 1 the velocities given are in meters/sec. The discrepancies between the theoretical and experimental velocities may be explained at least in part by the finite size of the impact tubes used to measure the velocity profiles. Thus it was not ΔP_w that could be measured, but some ΔP, at a point not on the wall, which was too low.

Considerable effort was expended in trying to force one of the "higher-order" modes of flow to appear, for which $n > 0$, but these experiments failed. The velocity profile for the $n = 1$ mode is shown in Fig. 4. The general method of attack on this problem was to try to

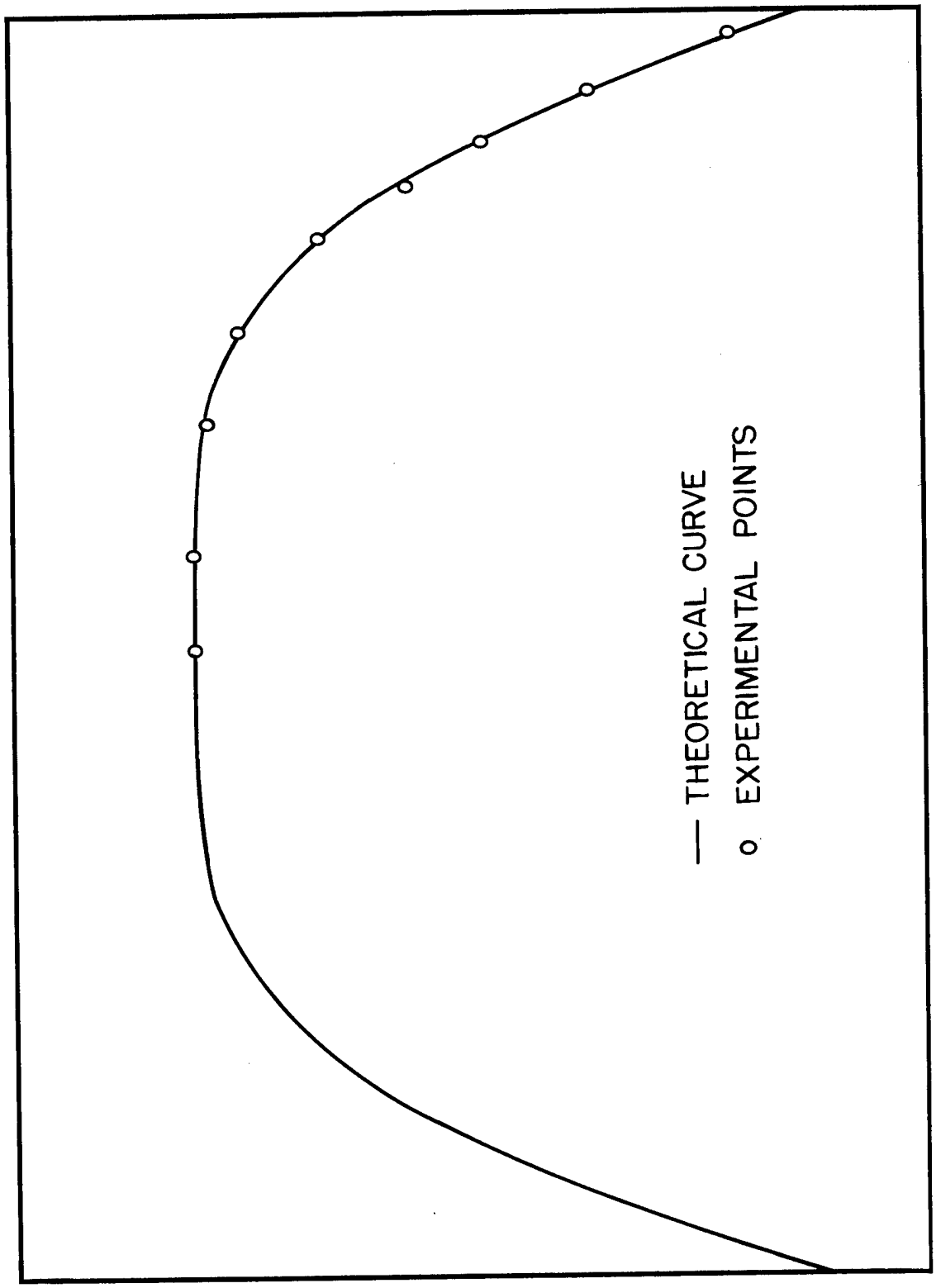

Fig. 3 - Velocity Profile for the n = 0 Mode

TABLE 1

VELOCITY PROFILE DATA ANALYSIS

ΔP_w	Q	$\frac{z}{L}$	v_{o_t}	v_{o_e}	$\sqrt{(\Delta P_w - \Delta P_r)/\Delta P_w}$							
3.61	12.3	1.00	17.1	16.2	0	0.103	0.392	0.566	0.675	0.807	0.932	0.974	1.000
9.01	30.8	1.00	42.8	40.5	0	0.091	0.359	0.556	0.674	0.789	0.921	0.970	1.000
11.11	37.9	1.00	52.7	49.9	0	0.147	0.370	0.540	0.660	0.803	0.930	0.977	1.000
6.11	23.2	0.90	29.0	27.5	0	0.216	0.406	0.588	0.679	0.805	0.937	0.987	1.000
5.44	23.3	0.80	25.9	24.5	0	0.252	0.399	0.576	0.687	0.817	0.934	0.987	1.000
4.81	23.4	0.70	22.8	21.6	0	0.275	0.402	0.590	0.689	0.817	0.937	0.978	1.000
3.35	18.2	0.63	15.9	15.1	0	0.247	0.410	0.590	0.719	0.830	0.938	0.990	1.000
6.81	36.8	0.63	32.2	30.6	0	0.295	0.421	0.572	0.688	0.811	0.923	0.990	1.000
10.37	56.0	0.63	49.0	46.6	0	0.306	0.414	0.575	0.689	0.814	0.941	0.990	1.000
					r (in 1/64")	48	46	42	38	35	31	24	17	7
					$\cos\left\{\frac{\pi}{2}\left[\frac{r}{a}\right]^2\right\}$	0	0.128	0.360	0.553	0.671	0.804	0.924	0.981	0.999

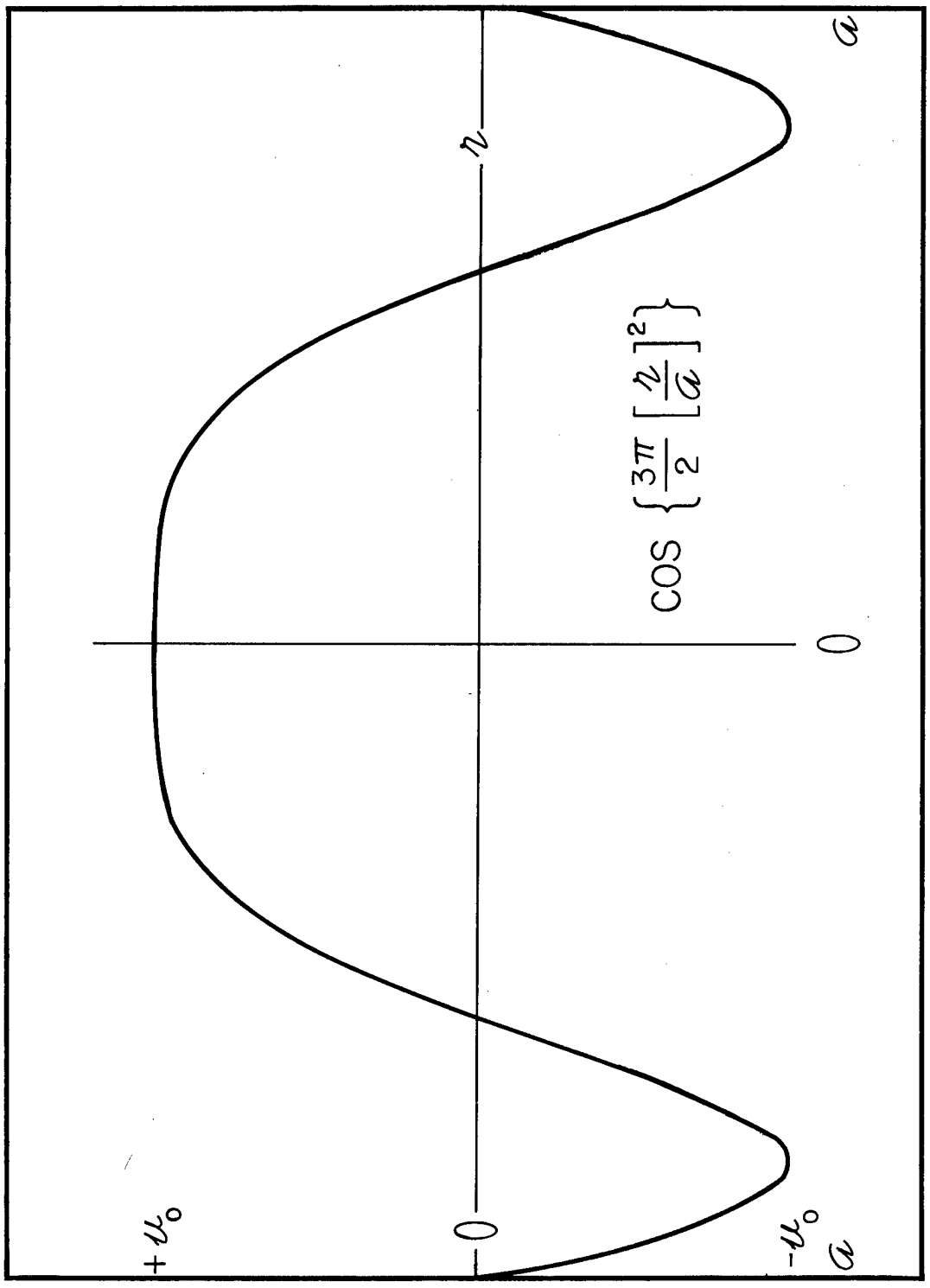

Fig. 4 - Theoretical Velocity Profile for the n = 1 Mode

control the exit boundary conditions so they would be favorable for the establishment of the desired flow scheme. The shape of the stream function was calculated and a plug which fit this function was machined and inserted into the gas stream. Since the experiments failed it has not been determined whether or not these "higher-order" solutions have physical significance.

It is interesting to note that the equations of motion that are solved are those that govern laminar, incompressible fluid flow, while the experiments were performed at exit Reynolds numbers high enough (up to about 100,000) that turbulence should have been well established, and with nitrogen, a compressible gas, as a working fluid. This indicates that the transition from laminar to turbulent flow either takes place only at even higher Reynolds numbers, or has little effect on the velocity profile.

Compressibility effects were quite small under the conditions used in our experiments. The maximum Mach numbers attained were 0.16.

REFERENCES

(1) J. R. Sellars, J. Appl. Phys. 26, 489 (1955).

(2) S. W. Yuan and A. B. Finkelstein, Trans. Am. Soc. Math. Engrs. 78, 719 (1956).

(3) M. Morduchow, Quart. Appl. Math. XIV, 361 (1957).

(4) A. S. Berman, Proc. 2nd Intern. Conf. Peaceful Uses Atomic Energy, Geneva, Paper No. P/720, vol. 4, p. 351, United Nations, New York (1958).

(5) F. M. White, B. F. Barfield, and M. J. Goglia, J. Appl. Mechanics 25, 613 (1958).

(6) H. L. Weissberg, Phys. Fluids 2, 510 (1959).